Identifying main uncertainties in estimating past and present radiative forcing of peatlands

Mathijssen, Paul J. H.

2022-07

Mathijssen , P J H , Tuovinen , J-P , Lohila , A , Väliranta , M & Tuittila , E-S 2022 , ' Identifying main uncertainties in estimating past and present radiative forcing of peatlands ' , Global Change Biology , vol. 28 , no. 13 , pp. 4069-4084 . https://doi.org/10.1111/gcb.16189

http://hdl.handle.net/10138/344516
https://doi.org/10.1111/gcb.16189

Received: 6 November 2021 | Revised: 24 February 2022 | Accepted: 21 March 2022

DOI: 10.1111/gcb.16189

RESEARCH ARTICLE

Global Change Biology WILEY

Identifying main uncertainties in estimating past and present radiative forcing of peatlands

Paul J. H. Mathijssen[1] | Juha-Pekka Tuovinen[2] | Annalea Lohila[2,3] | Minna Väliranta[4] | Eeva-Stiina Tuittila[5]

[1]Ecohydrology and Biogeochemistry Group, Institute for Landscape Ecology, University of Münster, Münster, Germany

[2]Climate Change Research, Finnish Meteorological Institute, Helsinki, Finland

[3]Institute for Atmospheric and Earth System Research (INAR)/Physics, University of Helsinki, Helsinki, Finland

[4]Environmental Change Research Unit, Ecosystems, Environment Research Program, Faculty of Biological and Environmental Sciences, University of Helsinki, Helsinki, Finland

[5]School of Forest Sciences, University of Eastern Finland, Joensuu, Finland

Correspondence

Paul J. H. Mathijssen, Ecohydrology and Biogeochemistry Group, Institute for Landscape Ecology, University of Münster, Münster, Germany.

Email: paul.mathijssen@uni-muenster.de

Funding information

Academy of Finland, Grant/Award Number: 296423, 330840 and 337550; Helsingin Yliopisto; Finnish Cultural Foundation; Ministry of Transport and Communication, Grant/Award Number: ICOS-ERIC: 281250 and ICOS-Finland: 281255

Abstract

Reconstructions of past climate impact, that is, radiative forcing (RF), of peatland carbon (C) dynamics show that immediately after peatland initiation the climate warming effect of CH_4 emissions exceeds the cooling effect of CO_2 uptake, but thereafter the net effect of most peatlands will move toward cooling, when RF switches from positive to negative. Reconstructing peatland C dynamics necessarily involves uncertainties related to basic assumptions on past CO_2 flux, CH_4 emission and peatland expansion. We investigated the effect of these uncertainties on the RF of three peatlands, using either apparent C accumulation rates, net C balance (NCB) or NCB plus C loss during fires as basis for CO_2 uptake estimate; applying a plausible range for CH_4 emission; and assuming linearly interpolated expansion between basal dates or comparatively early or late expansion. When we factored that some C would only be stored temporarily (NCB and NCB+fire), the estimated past cooling effect of CO_2 uptake increased, but the present-day RF was affected little. Altering the assumptions behind the reconstructed CO_2 flux or expansion patterns caused the RF to peak earlier and advanced the switch from positive to negative RF by several thousand years. Compared with NCB, including fires had only small additional effect on RF lasting less than 1000 year. The largest uncertainty in reconstructing peatland RF was associated with CH_4 emissions. As shown by the consistently positive RF modelled for one site, and in some cases for the other two, peatlands with high CH_4 emissions and low C accumulation rates may have remained climate warming agents since their initiation. Although uncertainties in present-day RF were mainly due to the assumed CH_4 emission rates, the uncertainty in lateral expansion still had a significant effect on the present-day RF, highlighting the importance to consider uncertainties in the past peatland C balance in RF reconstructions.

KEYWORDS

greenhouse gas balance, Holocene, lateral expansion, net carbon balance, peatland fires, peatland-climate feedback, radiative forcing

1 | INTRODUCTION

Peatlands constitute an effective sink of atmospheric carbon dioxide (CO_2), but they are also an important source of methane (CH_4; Korhola et al., 2010; Petrescu et al., 2015; Yu, 2011) and, under some circumstances, nitrous oxide (N_2O; Freeman et al., 1993; Langeveld et al., 1997; Martikainen et al., 1993; Repo et al., 2009). The exchange of these greenhouse gases (GHGs) between peatlands and the atmosphere has a dualistic effect on the climate, as one GHG (CO_2) is removed from the atmosphere while others are emitted. The current yearly CO_2 uptake by northern high latitude peatlands amounts to 40–66 Tg (Tg = 10^{12} g) of carbon (C; Turunen et al., 2002; Yu, 2011). During the Holocene (the last ca. 11,700 year), northern peatlands have accumulated over 500 Pg C (Pg = 10^{15} g), which is equivalent to the pre-industrial atmospheric C reservoir. Simultaneously, CH_4 losses to the atmosphere account for a significant proportion, up to 25%, of the net ecosystem C balance of peatlands (Limpens et al., 2008), adding up to ca. 15 Tg CH_4-C year^{-1} (Mikaloff-Fletcher et al., 2004). The magnitude of the CO_2 sink and CH_4 source has varied throughout the Holocene (Yu, 2011). This is due to the peatland GHG fluxes being regulated by not only autogenic peatland succession (Juottonen et al., 2021; Leppälä, Laine, et al., 2011; Leppälä, Oksanen, et al., 2011) but also to a great extent by climatic factors such as temperature, humidity, insolation, and precipitation (Dorrepaal et al., 2009; Fan et al., 2013; Gorham, 1991). Hence, to understand the role and feedback mechanisms of peatlands in the past global climate system, we need to assess their GHG exchange over the Holocene.

The climatic effect of peatland GHG fluxes can be expressed as radiative forcing (RF; Frolking et al., 2006), which is defined as the change in the global radiative balance (energy flux per area of Earth's surface, W m^{-2}). GHG emissions increase atmospheric GHG concentrations reducing the energy radiating to space; hence, this is defined as a positive RF that results in climate warming (Myhre et al., 2013). Removal of GHGs from the atmosphere has the opposite effect, that is, a negative RF resulting in climate cooling. RF depends not only on the magnitude of the GHG flux in question but also substantially on the radiative efficiency and time scales related to biogeochemical cycling of the GHG. This is especially relevant when comparing CO_2 uptake, which is associated with sustained forcing even when occurring in the short term, and a CH_4 emission pulse resulting in only a transient effect (Frolking et al., 2006).

The majority of northern peatlands initiated during the early Holocene, and their uptake and storage of CO_2 since then have affected atmospheric CO_2 concentrations (Yu, 2011). Several studies have reconstructed northern peatland GHG fluxes since the start of the Holocene (Gorham, 1991; Yu, 2011, 2012; Yu et al., 2010), but few have considered the RF associated with these fluxes (Frolking & Roulet, 2007; Mathijssen et al., 2014, 2017; Piilo et al., 2020). Frolking and Roulet (2007) estimated the RF associated with the development of northern peatlands throughout the Holocene, assuming linear peat expansion after initiation dates and various scenarios of CH_4 emissions, resulting in a current RF of −0.22 to −0.56 W m^{-2}. However, peatlands do not exhibit such linear lateral expansion after initiation (Mäkilä, 1997; Mathijssen et al., 2014, 2016; Piilo et al., 2020), and GHG fluxes per unit peat area are not constant through time (Mäkilä, 1997). When studying individual peatlands, it is possible to reconstruct peatland vertical and lateral growth and GHG fluxes in more detail (Loisel & Yu, 2013; Mäkilä, 1997; Mäkilä & Moisanen, 2007; Mathijssen et al., 2014, 2016, 2017), which can be used to calculate site-specific RF trajectories since peat initiation (Dommain et al., 2018; Mathijssen et al., 2017; Piilo et al., 2020).

In general, peatland RF will turn negative eventually due to sustained CO_2 uptake, overcoming the positive RF of CH_4 emissions. Assuming no variations in the fluxes or atmospheric conditions, the timing of this so-called switchover time only depends on the ratio between CO_2 and CH_4 fluxes (Frolking et al., 2006). Standardized to peatland area, estimates of northern peatland RF (Frolking & Roulet, 2007) collectively amount to −0.55 to −1.9 nW m^{-2} per ha of peatland (nW = 10^{-9} W), while the site-specific RF ranges from −3.3 to +0.6 nW m^{-2} ha^{-1} (Dommain et al., 2018; Mathijssen et al., 2016, 2017; Piilo et al., 2020).

Uncertainties in reconstructions of peatland C exchange can be divided into uncertainties pertaining to the net CO_2 exchange (as the product of CO_2 uptake and release) and CH_4 emissions. CO_2 uptake reconstructions are commonly deduced from the amount of C stored in peat layers of varying ages, assuming that the organic material that was formed when a certain layer was at the surface stays in place after that layer is buried under younger peat layers. It is common practice not to directly measure the C content throughout a peat profile. Instead, the proportion of organic matter is analysed, which is then multiplied with an assumed C content of organic matter (Loisel et al., 2014). However, the organic matter C content varies from 42% to 57% depending on peat type and decomposition state (Beilman et al., 2009; Loisel et al., 2014).

Estimation of all these C fluxes, that is, CO_2 uptake, CO_2 release and CH_4 emissions, is additionally affected by uncertainties in the areal development of a peatland, which is commonly reconstructed by interpolating areal growth between peat initiation and the present-day peatland size (Korhola, 1994). Variability in expansion rate is then based on the age and distribution of multiple basal peat ages (Mathijssen et al., 2016). This approach relies on the accurate localization of the oldest part of the peatland and a sufficiently large number of basal ages evenly distributed across the present-day peat area. Furthermore, any location where the peat layer has disappeared at any point in the past cannot be considered.

In paleoecological peatland studies, the long-term C fluxes are commonly summarized as apparent C accumulation rates (aCAR; g C m^{-2} year^{-1}; Loisel et al., 2014), calculated as the cumulative C stored between two peat layers of known age. However, the actual peat C balance at any given time is the result of both C uptake by vegetation at the peat surface, and C loss from all the peat layers that existed at that time. Even though the actual peat C balance were temporarily negative, that is, C loss from all layers is larger than uptake at the surface, the aCAR would always remain positive and average out any variability of the C balance over time (Frolking et al., 2014), in addition to overestimating recent C uptake rates (Young et al., 2019). However, a paleo-reconstruction of the peatland net C balance (NCB) can be modelled using aCAR as the present-day end result of past C uptake and subsequent decomposition with a constant loss rate (Yu, 2011). Additional uncertainties in C balance reconstructions stem from disturbances, such as peat fires (Loisel et al., 2017; Turetsky & Wieder, 2001), and loss of dissolved organic C through lateral water flow (Evans et al., 2016).

One of the main uncertainties in reconstructions of past peatland C dynamics is the estimation of past CH_4 emissions (Loisel et al., 2017). However, as a consequence of its relationship with vegetation characteristics, it is possible to reconstruct CH_4 emissions by using fossil plant species assemblages as proxy (Mathijssen et al., 2016), similar to the use of vegetation as an indicator for current CH_4 fluxes (Bubier et al., 1995; Couwenberg et al., 2011; Gray et al., 2013). However, the uncertainty in such CH_4 flux predictions often exceeds 50% (Bubier et al., 1995; Mathijssen et al., 2016). Another way to estimate peatlands' past CH_4 emissions is to determine their past type and trophic state and assume a typical flux rate as observed in similar peatlands at present (Mathijssen et al., 2014, 2017; Piilo et al., 2020). The main sources of uncertainty here would be the variability in observed flux rates and their temporal representativeness at the study site.

Several data compilations have been undertaken to synthesize global or continental-scale reconstructions of peatland development and their effect on the C cycle (Kleinen et al., 2012; Korhola et al., 2010; Yu, 2011). However, the Holocene reconstructions of northern peatlands and their climate effects have been performed based on either limited data of peatland C dynamics and lateral expansion patterns (Wang et al., 2009) or simulated data (Frolking & Roulet, 2007). Thus, before upscaling site-scale reconstructions, it would be prudent to investigate the uncertainties involved in them.

This study aims to quantify the relative uncertainties in RF pertaining to the varying assumptions necessary in reconstructions of peatland C dynamics and to assess how these assumptions relate to the interpretation of peatland-climate feedbacks. For that, we have selected three sites for which RF has previously been calculated throughout their entire development based on long-term estimates of C uptake, CH_4 emission and the lateral growth of peat surface.

2 | METHODS

2.1 | Approach

In this study, we focused on three Finnish peatlands for which the C dynamics and RF have recently been reconstructed throughout the Holocene (Mathijssen, 2016; Mathijssen et al., 2014, 2016, 2017). While the sites are characterized by relatively low overall C accumulation rates (Mathijssen et al., 2014, 2016, 2017), they are representative to the variation in northern peatlands in their vegetation and ecohydrology (Rydin & Jeglum, 2013). For our purposes they provide a useful sample because data collection methods and the assumptions inherent in their reconstructions of C dynamics were comparable. Furthermore, these three sites are some of the few for which Holocene-scale C and RF dynamics have been reconstructed (but see Dommain et al., 2018; Piilo et al., 2020).

To address our aim, we limit our study to the empirical data available for our sites; that is, we did not test the effect of having more or fewer measurement data. Consequently, we do not aim at providing 'best practice' guidelines on C dynamics measurements for RF reconstructions that would be better fitted to a modelling study.

The calculation of RF over the development history of each peatland was based on the reconstructed CO_2 uptake and CH_4 emission rates and peat area development, that is, lateral expansion, which were spatially integrated into annual peatland-scale CO_2 and CH_4 fluxes. In this paper, we refer to the CO_2 uptake and CH_4 emission rates expressed per unit area as 'flux densities' (g C m^{-2} $year^{-1}$) and use the term 'flux' (g C $year^{-1}$) for the rate of peatland-scale C exchange. In the original, site-specific studies, the reconstructed CO_2 uptake was assumed to equal aCAR, and the estimates of reconstructed CH_4 emission and lateral expansion were based on vegetation composition and linear interpolation between basal dates, respectively (Mathijssen et al., 2014, 2016, 2017). However, the uncertainties of these reconstructions were not translated into uncertainties of RF. To understand how the uncertainties involved in the reconstructions of CO_2 and CH_4 fluxes and lateral expansion affect the resulting RF, here the RF from peat initiation to 0 cal. year BP (before present, i.e., 1950 AD) was recalculated for these peatlands using varying approaches. In each approach, the empirical data underlying the original reconstructions were kept constant; that is, C-contents, age-depth models, vegetation composition, number, and age of basal peat samples were the same as in the original studies (Mathijssen et al., 2022). For all three variables (i.e., CO_2 and CH_4 fluxes and lateral expansion), we implemented three different reconstruction methods: the reconstructed CO_2 fluxes were based either on aCAR, net carbon balance (NCB) or NCB plus the C loss due to fires; CH_4 fluxes had 'minimum', 'average,' and 'maximum' emission variants; peat area was assumed to have had an 'early', 'expected' or 'delayed' expansion compared with the best estimate derived from observed basal ages. We followed the micrometeorological sign convention for CO_2 and CH_4 fluxes: a positive sign indicates a flux from the ecosystem to the atmosphere (emission) and a negative sign a flux from the atmosphere to the ecosystem (uptake).

2.2 | Study sites

Siikaneva (SII) is an open peatland of ca. 12 km^2 in southern Finland (61°50′N, 24°12′E, 160 m a.s.l.). The peatland, with its depth ranging from 2 to 6 m, contains bog and oligotrophic fen areas, of which the latter form the majority. Peat accumulation started ca. 11 kyr BP (kyr = 1000 years), and in some areas the plant composition shifted toward bog vegetation ca. 4.4 kyr BP. During its development, Siikaneva is estimated to have accumulated 970 Gg C (Gg = 10^9 g; Mathijssen et al., 2016). More information on the site in terms of vegetation and contemporary C dynamics can be found in Mathijssen et al. (2016), Aurela et al. (2007), Riutta et al. (2007), Rinne et al. (2007), Laine et al. (2012), Korrensalo et al. (2018) Männistö et al. (2019) and Alekseychik et al. (2021).

Kalevansuo (KAL) is also situated in southern Finland (60°39′N, 24°21′E, 123 m a.s.l.). It is a nutrient poor dwarf-shrub pine bog of 0.9 km^2, drained for forestry in 1969. Peat accumulation started ca. 10.5 kyr BP and resulted in a peat layer of 0.4 to 3 m, containing in total 44 Gg C (Mathijssen et al., 2017). Macrofossil evidence shows that most of the present peat area originally consisted of vegetation typical of a rich fen, which transformed into a poor fen, and finally into a bog state (Mathijssen et al., 2017). Only the peatland development up until the drainage is taken into account in this study. Additional information on Kalevansuo can be found in Mathijssen et al. (2017), Badorek et al. (2011), Koskinen et al. (2014), Lohila et al. (2011), Ojanen et al. (2012), Pihlatie et al. (2010) and Minkkinen et al. (2018).

Lompolojänkkä (LOM) is a narrow, nutrient-rich sedge valley fen with a relatively strong stream impact in the aapa-mire region of northern Finland (68°00′N, 24°13′E, 269 m a.s.l.). The fen of ca. 14 ha has a maximum depth of 2.5 m. Peat accumulation started at ca. 10 kyr BP, and the peatland vegetation has resembled a minerotrophic fen throughout its development (Mathijssen et al., 2014). Additional information on the contemporary C exchange at LOM can be found in Aurela et al. (2009, 2015) and Zhang et al. (2020).

2.3 | Carbon dioxide flux

In all our CO_2 flux reconstruction approaches, the CO_2 that was taken up and subsequently lost by the peatland in the form of CH_4 emissions or lateral flow was not considered to be contributing to the atmospheric CO_2 store, that is, we assumed that the C in CH_4 emissions and dissolved in lateral flow originated mainly from the recently assimilated CO_2 (Cooper et al., 2017) and that both rapidly return to the atmosphere as CO_2 (Evans et al., 2016; Frolking et al., 2006). All the approaches used for CO_2 flux reconstruction were constrained in their present-day total accumulated C uptake by the cumulative C observed in peat cores at the time of sampling, and thus the present-day C stocks of the sites did not differ between these approaches.

2.3.1 | Apparent carbon accumulation rate

Peat cores down to the peat base were radiocarbon dated and analysed for C content and bulk density (for details, see Mathijssen et al., 2014, 2016, 2017). Based on these data, the aCAR (g C m^{-2} $year^{-1}$) was calculated using

$$\mathrm{aCAR} = \mathrm{PAR} \times \rho \times c, \tag{1}$$

where PAR (m $year^{-1}$) is the peat accumulation rate resulting from age-depth models of the radiocarbon ages, ρ (g m^{-3}) is peat bulk density, and c (g C g^{-1}) is bulk peat C content.

The calculation of aCAR was performed for two peat cores from SII, eight cores from KAL, and one core from LOM. In the case of LOM, the aCAR flux densities (g C m^{-2} $year^{-1}$) were multiplied by the reconstructed peatland area (see below) leading to peatland C fluxes (g C $year^{-1}$) that were converted to CO_2 flux (g CO_2 $year^{-1}$; Mathijssen et al., 2014). In the cases of SII and KAL, with multiple aCAR records from various locations within the site, the aCAR flux densities were averaged and multiplied by peat area, taking into account the different successional stages across the site (Mathijssen et al., 2017); that is, the aCAR values from the bog-vegetation stage at SII were applied only to the bog area present at that time, while the flux densities from the other core from SII containing fen-vegetation were applied to the fen area of SII at that time (Mathijssen et al., 2016).

2.3.2 | Net carbon balance

We applied the NCB model (Yu, 2011) to quantify the C uptake and total C loss through decomposition at any given time during peatland development. This approach was adapted for the use in this study by dividing the aCAR flux densities into 1000-year binned time intervals, multiplying these by the reconstructed peat area during the respective time interval, and using the products as a net peat C pool (NCP, Gg C kyr^{-1}). The NCP and a decay coefficient (α) of 0.0001 $year^{-1}$ (Clymo et al., 1998; Rydin & Jeglum, 2013) were then used to calculate the net C uptake (NCU) and net C release (NCR) following:

$$\mathrm{NCU}_t = \frac{\mathrm{NCP}_t}{e^{-\alpha t}}, \tag{2}$$

$$\mathrm{NCR}_t = \sum_{k=t}^{\text{initiation age}} \left(\frac{\mathrm{NCP}_k}{e^{-\alpha t}} - \frac{\mathrm{NCP}_k}{e^{-\alpha (t-1)}} \right), \tag{3}$$

in which NCU represents the initial C input into the catotelm and NCR represents the summed C release due to decomposition in all peat layers (k) present at time t. The NCB was then calculated as

$$\mathrm{NCB_t} = \mathrm{NCU_t} - \mathrm{NCR_t}. \tag{4}$$

2.3.3 | NCB combined with fire loss

The third approach to model past CO_2 fluxes assumed that C from organic matter buried in peat would not only be lost due to ongoing decomposition, but also by combustion in peat fires. The presence of charcoaled macrofossil remains was used as an indicator for past fires (Table 1; Mathijssen et al., 2016, 2017). This approach followed the NCB method with the following modification (NCB-F): time intervals during which a fire took place experienced a C loss of 2.0 kg C m^{-2} (4.0 kg C m^{-2} in case of multiple or severe fires; Benscoter & Wieder, 2003; Turetsky & Wieder, 2001), which was assumed to

TABLE 1 Fire occurrence based on the presence of macroscopic charcoal in peat samples

Time interval (kyr BP)	SII	KAL	LOM[a]
0–1	–	1 fire	–
1–2	–	–	–
2–3	–	–	–
3–4	1 fire	–	–
4–5	–	2 fires[b]	–
5–6	1 fire	2 fires[b]	–
6–7	1 fire	2 fires[b]	–
7–8	–	2 fires[b]	–
8–9	2 fires[b]	–	–
9–10	1 fire	–	–
10–11	–	–	–

[a]No charcoal was observed in Lompolojänkkä.

[b]Large amounts of charcoal were observed indicating multiple fires or a large fire event.

have been accumulated in the previous time interval. This meant that the burned and lost C was stored in the peatland for 1000 year.

2.4 | Methane emission

Our reconstructions of CH_4 emissions were based on contemporary CH_4 fluxes, which were then applied to the past by linking them to the reconstructed vegetation composition. The estimated CH_4 flux densities were also averaged over 1000-year intervals and multiplied by the corresponding reconstructed peatland areas. For SII, a weighted averaging transfer function was used to estimate the past emissions using plant macrofossils as input and chamber flux measurements with corresponding vegetation composition from SII and an additional site as a training set (Mathijssen et al., 2016). For SII, the 'average' CH_4 emission variant equalled the predicted emissions, while the 'minimum' and 'maximum' emission variants were defined as the predicted emissions minus and plus the sample-specific errors, respectively. For KAL, the peatland CH_4 flux was calculated from flux densities of subareas for which the development of peat type was described separately (Mathijssen et al., 2017). Each subarea was assumed to have a CH_4 flux density corresponding to peat type, following Minkkinen and Ojanen (2013), who collected contemporary CH_4 flux data of Finnish peatlands. The 'average' CH_4 emission variant used the mean contemporary flux density, while the 'minimum' and 'maximum' emission variants were defined as the mean minus and plus standard deviation, respectively. For LOM, site-specific contemporary CH_4 flux measurements were available (Mathijssen et al., 2014) and adopted for the 'average' CH_4 emission variant. The 'minimum' and 'maximum' emission variants were defined as the mean measured flux density in LOM minus and plus the standard deviation of the fluxes at Finnish-rich fens (Minkkinen & Ojanen, 2013), respectively.

2.5 | Peatland area

Reconstructions of peatland lateral expansion were based on the age of basal peat samples spread across each site (18 at SII, 19 at KAL and 9 at LOM). The 'expected' variant of peat area development consisted of the best estimate of expansion based on linear interpolation between basal ages, considering base morphology. This variant represented the reconstructions published previously (Mathijssen et al., 2014, 2016, 2017). The 'early' expansion variant assumed that lateral growth occurred as early as possible in the lifetime of the peatland while not contradicting the ages of the basal samples. Correspondingly, the 'late' variant assumed lateral growth to have occurred as late as possible.

2.6 | RF model

The peatland-scale CO_2 and CH_4 fluxes of the three sites were used to calculate the sites' RF during their development history. We used the sustained pulse-response model described by Lohila et al. (2010), Mathijssen et al. (2017) and Piilo et al. (2020) to calculate the RF resulting from the changes in atmospheric concentrations due to CO_2 and CH_4 exchange at the sites (RF_{CO2} and RF_{CH4}). This model has previously been applied for these sites (Mathijssen, 2016; Mathijssen et al., 2014, 2017), but here RF was recalculated because the model has been updated since these studies. This update included implementation of improved radiation efficiency functions, which increased the RF sensitivity to changes in atmospheric CH_4 concentration (Etminan et al., 2016). In addition, the updated version takes into account the variations in the background concentrations of the GHGs considered, that is, CO_2, CH_4 and N_2O (Köhler et al., 2017). For the purpose of this study, the fluxes were calculated in 1000-year intervals, and the yearly RF values modelled were averaged over these intervals. The RF model equations and parameter values are detailed in Supporting Information.

3 | RESULTS

3.1 | Peat expansion

The reconstructed peatland expansion, interpolated from the distribution of basal dates, showed different patterns between the three sites. In SII, peat growth started in several small loci between 11 and 10 kyr BP, after which the peat area expanded rapidly until 5 kyr BP and slowly after that (Figure 1a,d). The uncertainty in the expansion pattern in SII was most pronounced during 10–5 kyr BP (Figure 1d). In KAL, peat formation first initiated across an elongated region in the middle of the current peatland (Figure 1b), after which it expanded steadily over time. The relative uncertainty in the size of the KAL peatland area was highest at 8 kyr BP (Figure 1e). The expansion pattern of LOM contrasted with that of SII in that it contained a rapid peat establishment during 10–9 kyr BP, after which expansion slowed down,

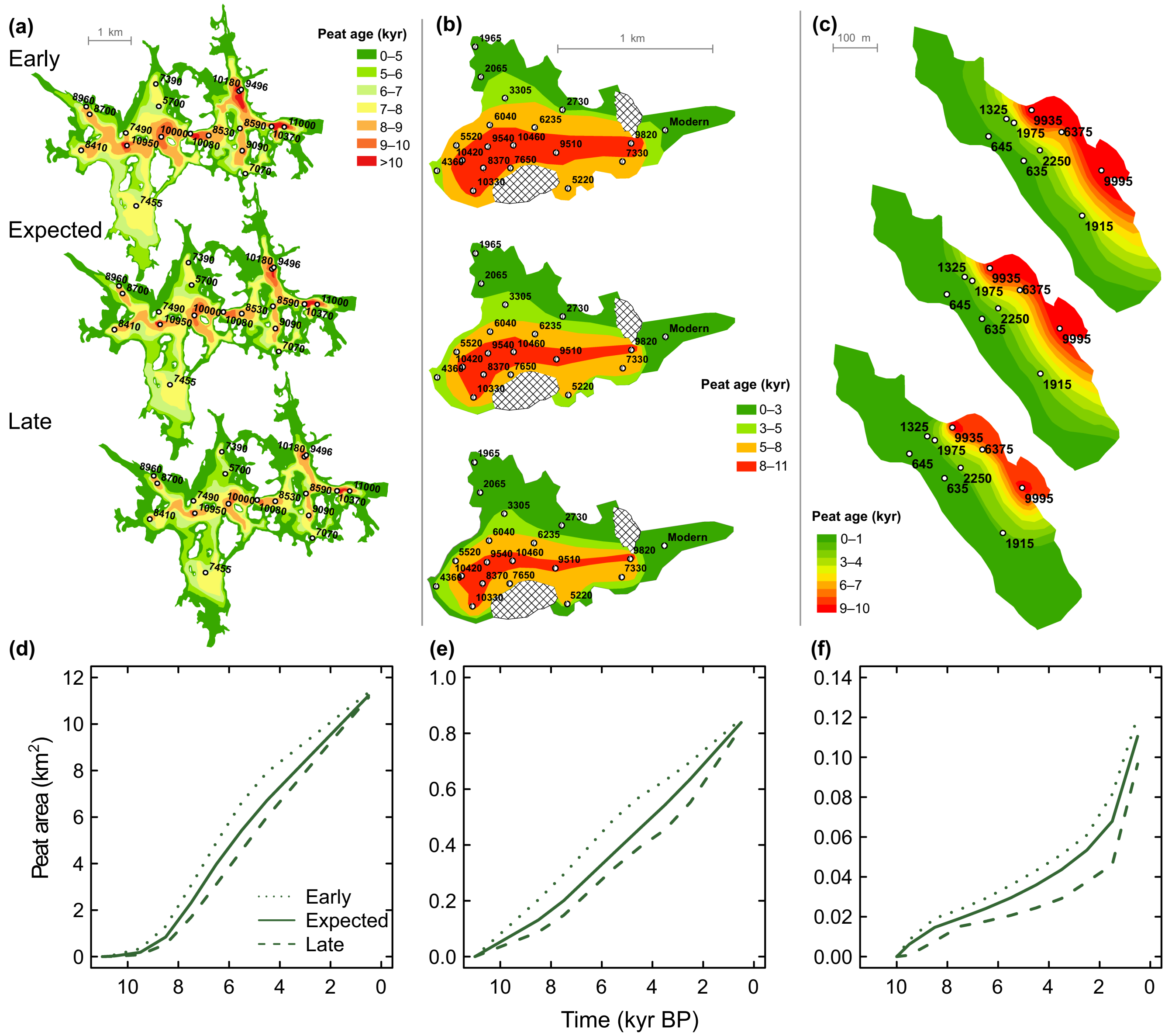

FIGURE 1 Reconstructed peatland expansion in Siikaneva (a), Kalevansuo (b), and Lompolojänkkä (c) assuming the 'best estimate' of expansion based on basal dates (expected), and early, and late expansion without contradicting basal dates. (d–f) Development of total peat area over the last 11,000 year for the respective sites

to increase rapidly after 2 kyr BP (Figure 1c,f). The deviation of the 'early' and 'late' expansion patterns from the best estimate ('expected') amounted to a maximum peat area uncertainty at any given time of +20% ('early') to −25% ('late') for SII, +30% to −50% for KAL and +20% to −30% for LOM (Figure 1d-f). The present-day C stock varied according to expansion patterns and reached 692, 615 and 562 Gg C for SII, 50, 44 and 39 Gg C for KAL and 4.0, 3.5 and 2.9 Gg C for LOM after 'early', 'expected' and 'late' expansion scenario, respectively.

3.2 | Carbon dioxide uptake

Using the aCAR approach, the CO_2 flux densities of all three peatlands were relatively stable throughout their development (Figure 2a–c), with faster CO_2 uptake either initially (LOM) or during the last 1000 year (KAL, LOM). LOM had the lowest uptake rate during most of the Holocene. At all sites, applying the NCB approach more than doubled the flux density estimate during the early phase of peatland development, while the following 1000 year periods showed a decreasing trend in the CO_2 uptake. For the last thousand years, the NCB approach decreased the estimated CO_2 uptake by up to 4.6 g CO_2-C m^{-2} year^{-1} (45%) compared with aCAR. The NCB-F approach, which assumes an additional burned C loss from SII and KAL, decreased the magnitude of reconstructed CO_2 flux density for the time intervals containing fires. However, NCB-F also raised the CO_2 uptake in the preceding intervals by up to 13 g CO_2-C m^{-2} year^{-1}, compensating for the subsequent C loss within a smaller peat area. This increased

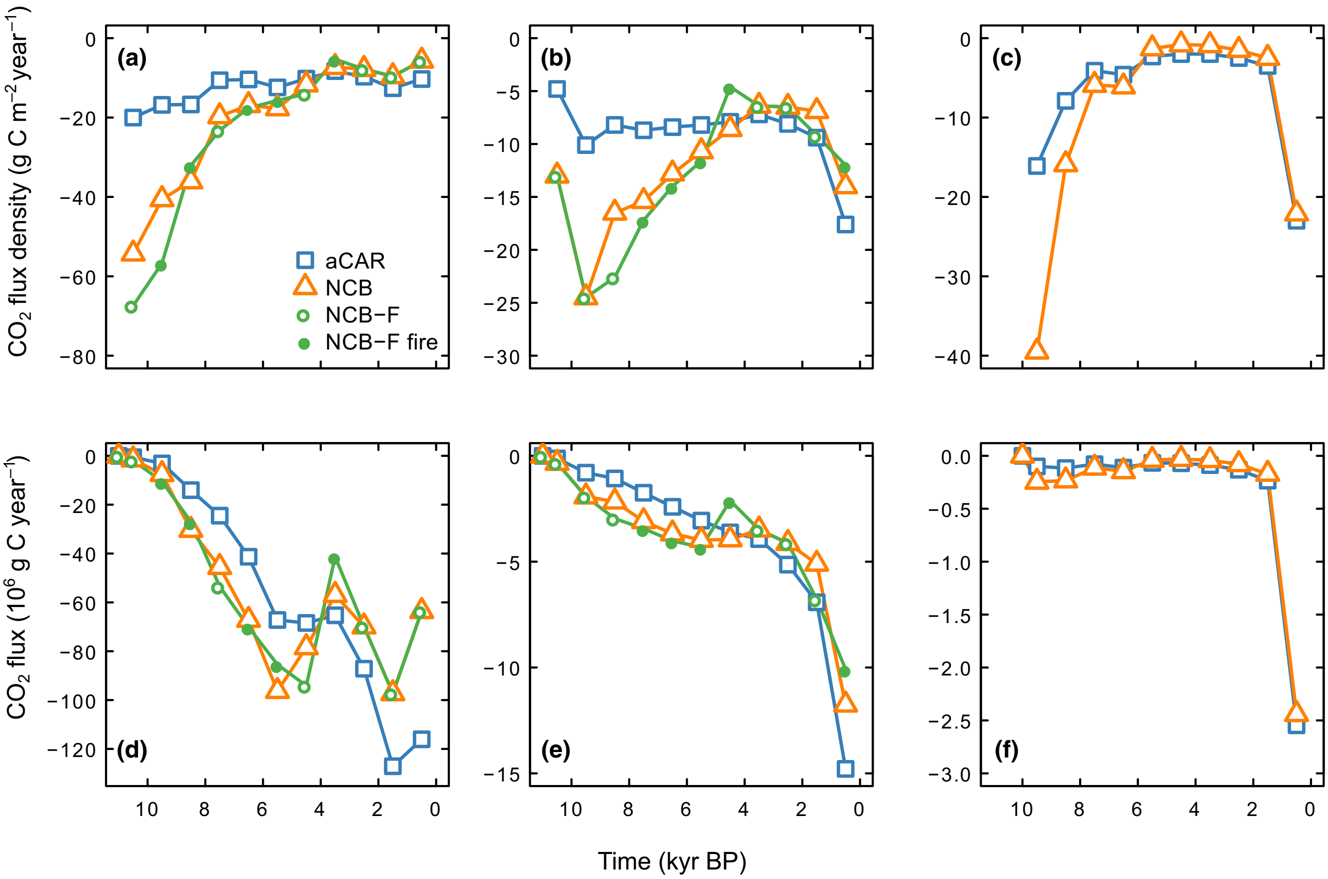

FIGURE 2 CO_2 flux density based on apparent C accumulation rate (*aCAR*, squares), net C balance (*NCB*, triangles), and NCB including fire effect (*NCB-F*, circles) in Siikaneva (a), Kalevansuo (b), and Lompolojänkkä (c). (d–f) Total peatland CO2 flux (flux density multiplied by expected peat area) of the respective sites. Filled circles indicate time intervals when fires occurred

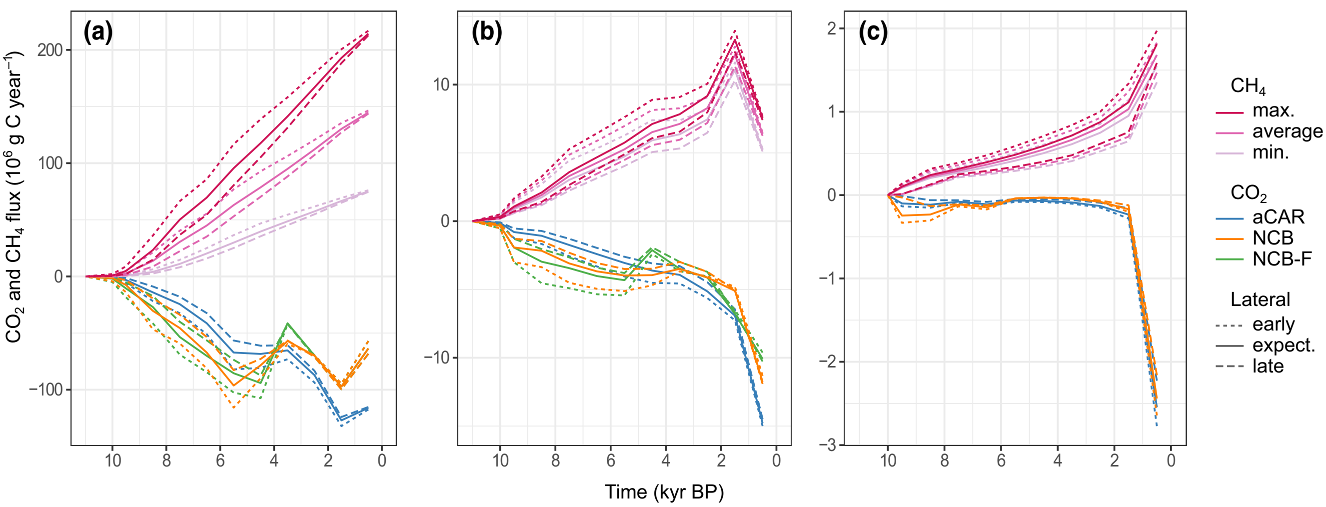

FIGURE 3 Site-scale CO_2 and CH_4 fluxes in Siikaneva (a), Kalevansuo (b) and Lompolojänkkä (c) depending on 'early' (*dotted*), 'expected' (*solid*) or 'late' (*dashed*) lateral expansion. The 'expected' fluxes are the same as depicted in Figures 2d–f and 4d–f

CO_2 uptake in the fire-preceding intervals elevated their CO_2 flux magnitude above that of the NCB approach, even when these intervals also contained fires (6–7 and 9–10 kyr BP in SII; 5–8 kyr BP in KAL; Figure 2d,e). During the majority of peatland development, the effect of varying the CO_2 flux reconstruction approach on the flux estimate was approximately double the effect of varying the lateral expansion pattern (Figure 3). In SII and KAL, the uncertainty related to the choice of the CO_2 flux reconstruction method increased further after 4 kyr BP, relative to that due to the expansion pattern estimation (Figure 3a,b).

3.3 | Methane emission

Translating the uncertainty of the plant composition-based reconstruction of CH_4 flux density into peatland-scale CH_4 fluxes in SII resulted in a late Holocene flux uncertainty ranging from 75 to 214 Mg CH_4-C year^{-1} (Figure 4d), while KAL and LOM inherited lower levels of uncertainty from the literature data, resulting in flux uncertainties from 5.2 to 7.5 and from 1.5 to 1.8 Mg CH_4-C year^{-1}, respectively, during the last millennium (Figure 4e,f). Succession from poor fen to bog across substantial parts of KAL since 2 kyr BP halved the CH_4 flux densities from 15–18 to 6–9 g CH_4-C m^{-2} year^{-1} (Figure 4b), which reduced the peatland-scale flux from 11–13 to 5.2–7.5 Mg CH_4-C year^{-1} (Figure 4e), even though peatland area was expanding (Figure 1e). Paleoecological evidence from LOM suggests that this site has remained a uniform rich fen throughout its history, and thus we assume that the CH_4 flux density has remained constant (Figure 4c). This means that variation in the peatland-scale flux was only controlled by areal expansion (Figure 4f). The dominant control of peat area development on CH_4 fluxes was illustrated in the combined effect of lateral expansion pattern and CH_4 flux density on the peatland-scale CH_4 flux in KAL and LOM (Figure 3b,c). SII was the exception because its uncertainty range in CH_4 flux density was more than four times as large as in KAL and LOM (Figure 4a–c).

3.4 | Radiative forcing

Earlier peatland expansion caused RF_{CO2} and RF_{CH4} to decrease and increase faster, respectively (Figure 5a–c), compared with 'expected' expansion. During the late Holocene, the difference in RF_{CH4} between different expansion pattern scenarios decreased, while this did not occur in RF_{CO2}, resulting in the net RF of the 'early' expansion scenario switching from being the most positive to the most negative (Figures 5d,e and 6). The current net RF, based on aCAR and average CH_4, equalled −270, −134 and −39 nW m^{-2} in SII, and −45, −34 and −26 nW m^{-2} in KAL, for the 'early', 'expected' and 'late' scenarios, respectively. However, in LOM the range of RF_{CO2} related to different expansion patterns remained smaller than that of RF_{CH4} (Figure 5c), and the current net RF equalled 6.4, 6.1 and 5.8 nW m^{-2} for the 'early', 'expected,' and 'late' scenarios, respectively.

The difference in RF_{CH4} corresponding to the 'min.', 'average' and 'max.' CH_4 emission scenarios followed the trajectories of CH_4 fluxes, maintaining the relationship RF_{CH4}('min.') < RF_{CH4}('average') < RF_{CH4}('max.') throughout peatland lifetime. At the maximum difference between the scenarios, the RF_{CH4} in SII equalled 500, 960 and 1430 nW m^{-2}, for 'min.,' 'average,' and 'max.', respectively, while in KAL the corresponding RF_{CH4} estimates were 35, 43 and 51 nW m^{-2}, and in LOM they were 10.2, 11.1 and 12.0 nW m^{-2} (Figure 5a–c).

The CO_2 fluxes estimated with the NCB method resulted in a negative RF_{CO2} that was decreasing faster compared with the aCAR approach, which lead to a lower NCB-based RF_{CO2} during the mid-Holocene (−292 vs. −487, −18 vs. −30 and −1.0 vs. −1.6 nW m^{-2} during 6–5 kyr BP for the 'expected' lateral expansion scenario in SII, KAL and LOM, respectively), after which the RF_{CO2} of aCAR and NCB approached each other again, showing only minor differences during the most recent 1-kyr period (Figure 6). The NCB-F approach produced RF_{CO2} trajectories that were very similar to those obtained using NCB (Figure 5a,b), with a maximum difference of 10%–15% during 9–5 kyr BP in KAL (Figure 5b,e).

In SII, the difference between the CH_4 flux reconstruction approaches was larger than that between the methods used to estimate CO_2 fluxes and lateral expansion (Figures 5d and 6). However, during 6–4 kyr BP, the difference between aCAR and NCB approached the same order of magnitude as between the 'average' and 'max.' CH_4 scenarios. The maximum uncertainty in net RF due to the uncertainty in lateral expansion of ca. 230 nW m^{-2}, and the maximum difference between aCAR and NCB of ca. 280 nW m^{-2}, were overshadowed by the maximum difference between the CH_4 flux estimates of ca. 940 nW m^{-2} (Figure 6a). The largest part of the overall uncertainty in net RF in KAL and LOM was due to the uncertainty in lateral expansion (maximum 20 and 2.5 nW m^{-2}, respectively; Figure 6b,c), while the maximum difference between different CO_2 flux estimates equalled 17 and 0.9 nW m^{-2} and that between different CH_4 fluxes 16 and 1.9 nW m^{-2}, in KAL and LOM, respectively.

4 | DISCUSSION

4.1 | Differences in original methods between sites

It is important to note, for the interpretation of the results of this study, that the exact methods used to reconstruct C fluxes differed among the three sites considered here. This is due to the fact that the original studies differed in their methods, as they attempted to make the most of the different types of data sets available for these peatlands. The studies of SII and KAL included data from multiple peat cores (Mathijssen et al., 2016, 2017), and thus the reconstructed flux densities were based on multiple locations within the site and took into account the relative distribution of peat types and its changes throughout the Holocene. In contrast, the data from LOM only included one peat core to base flux estimation on (Mathijssen et al., 2014), so we had to assume that this core was representative of the entire peatland.

The largest difference in methods between the sites occurs in the reconstruction of CH_4 emissions. While for KAL and LOM we had to rely on collated measurement data (Minkkinen & Ojanen,

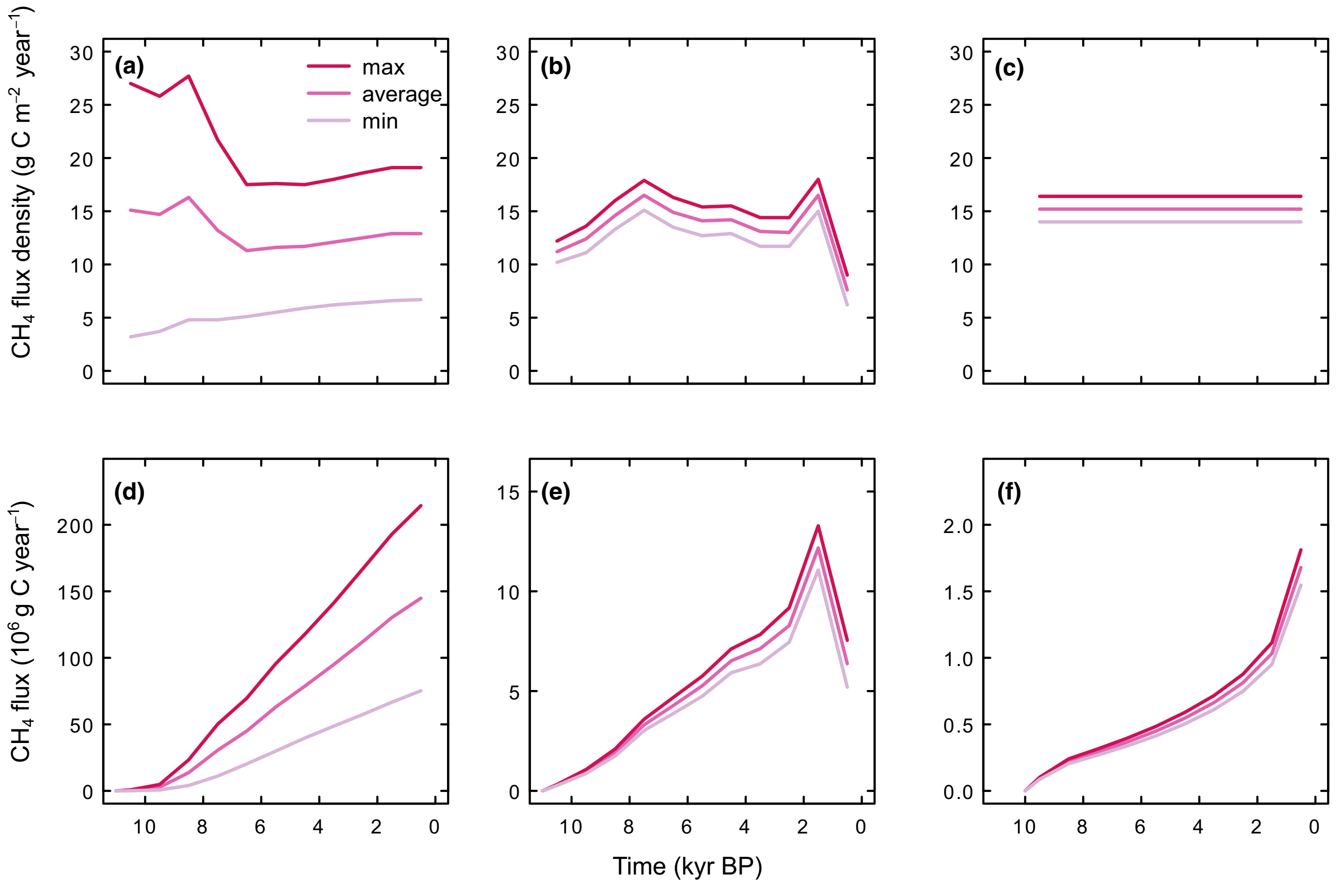

FIGURE 4 Methane flux density following assumptions of minimum, average and maximum methane emission for Siikaneva (a), Kalevansuo (b) and Lompolojänkkä (c). (d–f) Total peatland methane flux (flux density multiplied by expected peat area) of the respective sites

2013) and derive different scenarios from the variation in these data, with a difference between the scenarios ranging up to 3 g CH_4-C m^{-2} year^{-1} (Figure 4b,c), in SII an effort was undertaken to model the past CH_4 emissions using macrofossil composition, which resulted in flux density uncertainties of over 20 g CH_4-C m^{-2} year^{-1} (Figure 4a). The uncertainty in CH_4 flux density in KAL and LOM would be higher if we had taken into account that the mean fluxes from the collated data (Minkkinen & Ojanen, 2013) may not accurately represent these peatlands during their earlier development. As a result of this approach, SII had the largest uncertainties in CH_4 flux densities, even though the most detailed data were available from this site.

We retained these methodological differences between sites as our aim was to investigate how the uncertainties connected to reconstructions of past fluxes affect the reconstructed RF and not to compare the uncertainties among the three sites. However, we argue that each reconstruction approach can be considered a reasonable choice, and thus including various methods provides information on the range of uncertainties that should be considered when interpreting RF reconstructions and on how these uncertainties depend on the underlying site-specific data.

4.2 | Relative effect of uncertainties in CO_2 uptake, CH_4 emissions and lateral expansion

The uncertainty in the estimated CO_2 uptake rates had a strong impact on the modelled past RF, as indicated by the fact that during the early Holocene the NCB-based RF_{CO2} decreased faster than the RF_{CO2} calculated from aCAR data. Taking into account the temporary removal of CO_2 from the atmosphere increased the CO_2 uptake earlier in peatland development (before the subsequent C loss) and decreased them during the later stages (Figure 2). However, while the order of CO_2 flux magnitudes in different trajectories changed during the mid-Holocene—with higher early-Holocene fluxes obtained with NCB and NCB-F than aCAR, while the opposite is true for the late Holocene due to ongoing C loss from deep and old peat layers—a similar change did not occur in RF_{CO2} (Figure 6). This switch and the cumulative nature of the RF due to sustained uptake of atmospheric CO_2 uptake (Myhre et al., 2013) resulted in a convergence of the RF_{CO2} of the different CO_2 uptake approaches during the late Holocene and in a similar present-day RF_{CO2} for the aCAR, NCB and NCB-F approaches (Figure 5a–c). This convergence was to be expected because all CO_2 flux approaches were constrained by the present-day C stock.

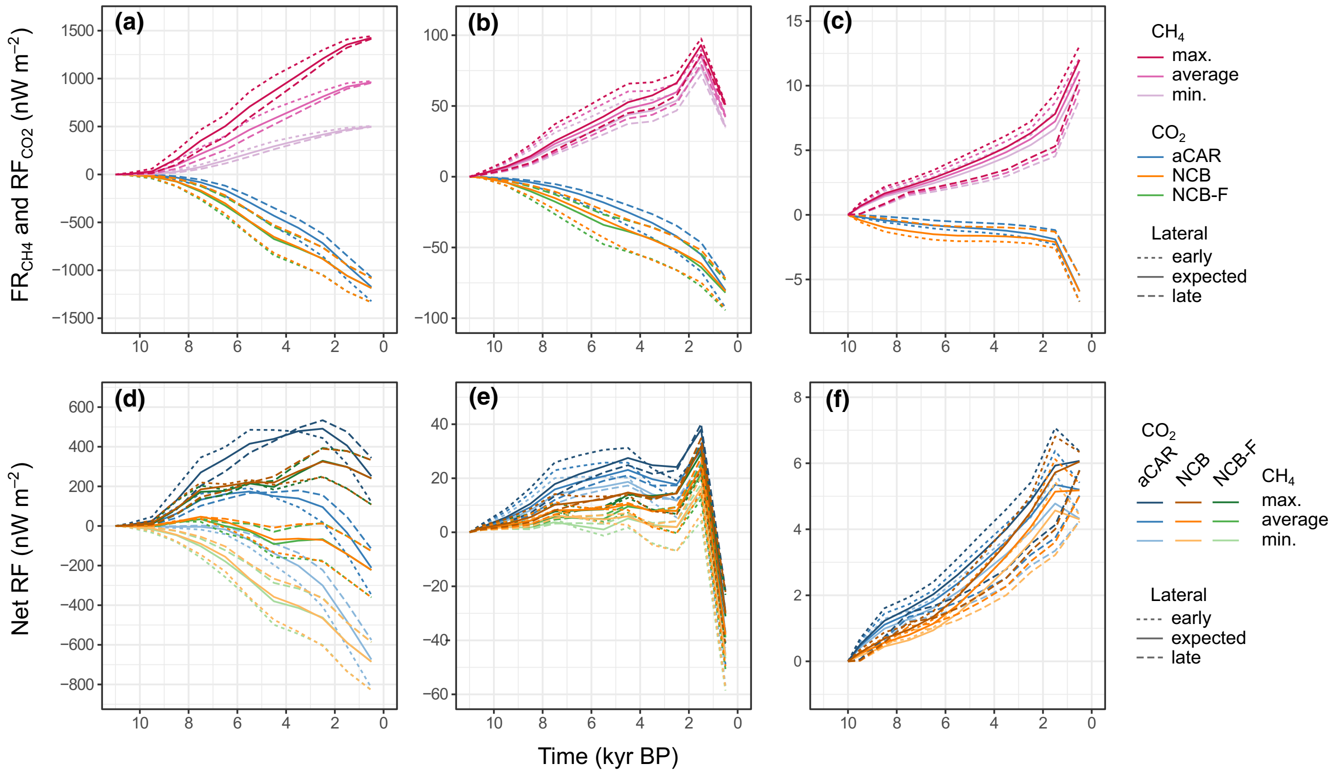

FIGURE 5 Radiative forcing of Siikaneva (a, d), Kalevansuo (b, e) and Lompolojänkkä (c, f). (a–c) RF due to the exchange of CO_2 (RF_{CO2}) and CH_4 (RF_{CH4}) for different approaches for CO_2 flux, CH_4 flux and lateral expansion reconstruction. (d–f) Net radiative forcing (sum of RF_{CO2} and RF_{CH4})

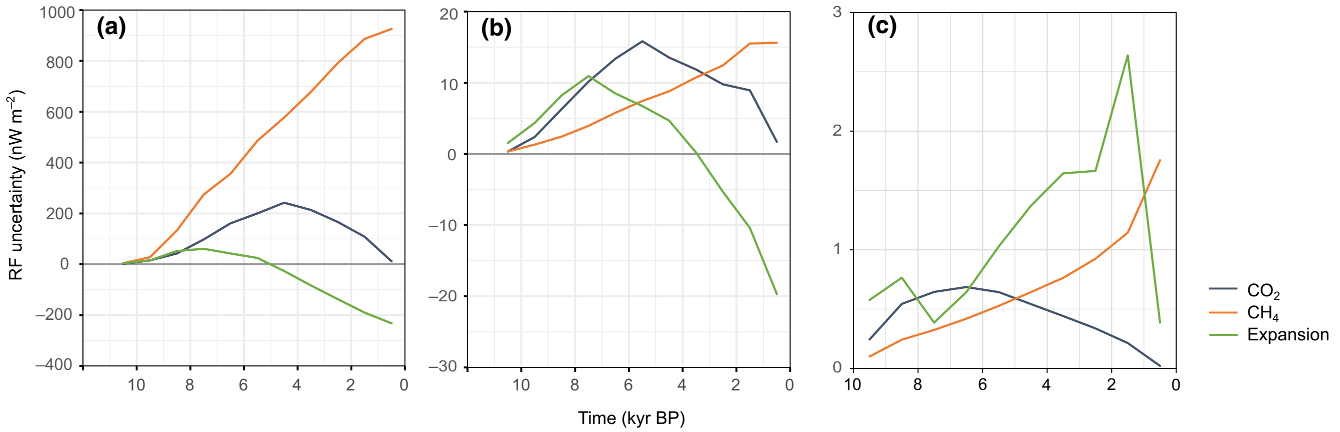

FIGURE 6 Radiative forcing uncertainty expressed as the difference between reconstruction approaches of CO_2 flux (maximum of apparent C accumulation rate [aCAR] minus net C balance [NCB] and aCAR minus NCB-F, with 'expected' expansion; blue line), CH_4 flux ('maximum' minus 'minimum', with 'expected' expansion; orange line) and lateral expansion ('early' minus 'late' expansion, with NCB and 'average' CH_4 flux; green line) in Siikaneva (a), Kalevansuo (b) and Lompolojänkkä (c)

The early-Holocene CO_2 fluxes had a large effect on the switchover time, that is, the time before the total RF turns negative, of the reconstructed peatlands. In the case of SII with 'average' CH_4 flux and 'expected' lateral expansion, it took from 11 kyr BP until 2 kyr BP before the net RF turned negative when using the aCAR approach (i.e., a switchover time of 9000 year), while with NCB or NCB-F this occurred at 6 or 7 kyr BP, respectively (Figure 5d), reducing the switchover time by 4000 to 5000 year. Uncertainties in the rate of lateral expansion likewise had large effects on the switchover times: SII with 'average' CH_4 flux and NCB resulted in switchover times of 4000 ('early'), 5000 ('expected') and 9000 year ('late'). However, taking into account the full uncertainty in CH_4 fluxes in SII would overshadow the effects of CO_2 flux reconstruction and lateral expansion approach, as using 'max.' and 'min.' CH_4 emission scenarios resulted in a net RF that was permanently positive or negative, respectively, and no switchover occurred in these cases. In KAL and LOM, the CO_2 flux and lateral expansion scenarios had only a minor effect on the switchover, since its timing was predominantly dependent on a rapid decrease in CH_4 fluxes since 2 kyr BP (KAL; Figure 5b,e), or no switchover occurred at all (LOM; Figure 5f).

Although the effect of fires on CO_2 flux was substantial during the millennium in which the fire occurred (Figure 2), this effect was largely absent from the RF_{CO2} (Figure 5). The effect of the C lost during a fire on RF was smaller than the effect of the C uptake increase generated into the reconstruction of the previous time interval. For example, the C uptake estimate for SII during 8–9 kyr BP was reduced by 11% when replacing NCB by NCB-F, but the amount of C lost in fires would appear to have been taken up during 9–10 kyr BP, enhancing the earlier RF_{CO2} and resulting in a RF_{CO2} at 8–9 kyr BP that is more negative by 3%. In this sense, including C losses by peat fires, but maintaining the same overall cumulative C pool, slightly enhances the estimated cooling effect during a peatland's lifetime because the uptake of CO_2 occurred earlier. In the long term, this effect becomes insignificant after a few thousand years since the last fire (Figure 5). These findings are in line with those of Dommain et al. (2018), who found that fires would accelerate C losses from tropical peatlands but would not alter the conclusions about the development of RF.

Since a CH_4 emission pulse has a relatively short-term RF effect (Frolking et al., 2006), the instantaneous RF_{CH4} at any time is close to the equilibrium determined by the atmospheric perturbation time scale of CH_4 and the mean emission during a few decades before that time. This resulted in limited differences in RF_{CH4} between the different assumptions on peat area expansion (Figure 5) because all expansion scenarios were constrained to reach the current peatland size at 0 kyr BP (Figure 1). In contrast, RF_{CO2} was cumulatively affected by the expansion scenarios. The 'early' scenario involved more CO_2 sequestered from the atmosphere over the peatland lifetime, which had the lasting effect of a more negative RF (Figures 5 and 6). In terms of peat area, the 'early' and 'late' expansion scenarios deviated from the 'expected' scenario by 15%–32% at 6–5 kyr BP (ca. midpoint of each peatland lifetime). The resulting RF_{CO2} and RF_{CH4} were affected by 21%–44% and 15%–33% at this time, but only by 9%–21% and 1%–13% at 1–0 kyr BP, respectively. The varying assumptions of peat expansion affected the modelled timing of the net RF peak and the switchover time; in SII, for example, the peak shifted by 2000 to 3000 year and the switchover time was varied by 1000 year (Figure 5d).

Comparing the relative importance of different types of uncertainties on net RF, there is a clear distinction to be made between considering the present-day and mid-Holocene net RF. The present-day uncertainties due to CH_4 flux densities had the largest effect, followed by the estimation of lateral expansion and lastly the CO_2 flux approach (Figure 6). Only in KAL was the present-day uncertainty in RF_{CH4} reduced due to a recent transition from poor fen to bog (Mathijssen et al., 2017). The lower present-day relative uncertainties of expansion patterns and CO_2 flux can be explained by the fact that these are constrained by the present-day peat area and C stock, respectively, which are easily quantified. During the mid-Holocene, roughly at the midpoint of the study sites' development history, the CO_2 flux approach had the largest effect (NCB vs. aCAR) except in SII (Figure 6). There the uncertainty due to CH_4 flux scenario was dominant throughout the Holocene (Figure 6a). During the mid-Holocene, the effects of CO_2 flux, CH_4 flux and expansion approaches were of similar magnitude in KAL and LOM (Figure 6b,c), although the largest effect was due to either CO_2 flux (KAL) or expansion (LOM). In SII, the effect of the expansion approach remained smaller than that of CO_2 flux until ca. 2 kyr BP (Figure 6a). Furthermore, as RF_{CO2} and RF_{CH4} have opposite signs and both depend on the past trajectory of peatland area, in some cases the sign of net RF depends on the expansion approach adopted (Figure 5d,e) and thus the related uncertainty becomes insignificant at some point of time (Figure 6a,b).

The uncertainties stemming from the different approaches applied in this study to reconstruct the expansion and CO_2 and CH_4 fluxes of peatlands were larger than the uncertainties in the radiative efficiency parameterizations of our RF model, estimated at ca. 10% for CO_2 and 14% for CH_4 (Etminan et al., 2016), except in the case of the uncertainty in the present-day RF resulting from CO_2 flux approach. A previous RF reconstruction of a northern peatland showed similar results, where uncertain CO_2 fluxes during the early stages of peatland development had a lasting effect on the instantaneous RF induced much later (Piilo et al., 2020). Hence, these uncertainties should be taken into account when long-term RF reconstructions are interpreted.

4.3 | Impact on interpretation of peatland role in climate system

Assuming sustained and constant ecosystem-atmosphere exchange of CH_4 and CO_2, the ratio between CH_4 emission and CO_2 uptake determines how long it takes before the switchover from positive to negative RF takes place (Frolking et al., 2006). When we calculated the molar CH_4:CO_2 flux ratio (moles of CH_4 emitted per moles of CO_2 uptake) as the mean ratio between CH_4 and CO_2 fluxes from peat initiation until the switchover occurred, we found that with a CH_4:CO_2 ratio of 0.2 the switchover time was less than 1000 year (SII with aCAR and min. CH_4; Figure 5d). This corresponds to the results presented for a hypothetical peatland by Frolking et al. (2006). The CH_4:CO_2 ratios of 0.5 and 1.1 resulted in switchover times of ca. 6000 and 10,000 year, respectively (SII with NCB and average CH_4 and SII with aCAR and average CH_4, respectively), while a CH_4:CO_2 ratio larger than 1.5 would not result in a switchover within the whole peatland history, 11,000 year (SII with max. CH_4; LOM all cases). The switchover time of 6000 year is larger than that estimated by Frolking et al. (2006). In KAL, the switch from positive to negative RF was due to the large increase in CO_2 uptake during the last 1000 year (Figure 2b) rather than the cumulative effect of CO_2 uptake over time. Thus, in KAL the switchover time could not be related to the long-term CH_4:CO_2 ratio.

The uncertainties in RF observed in this study were similar to the uncertainty range presented by Frolking and Roulet (2007). However, when standardized to peat surface area, the individual sites studied here reached a much higher present-day RF of −0.7 to +0.6 nW m^{-2} per hectare of peatland, than −1.9 to −0.6 nW m^{-2} ha^{-1} for northern peatlands collectively, where the range represents various scenarios of constant CO_2 uptake and CH_4 emission over the Holocene (Frolking & Roulet, 2007). Part of this difference can be explained by differences in RF modelling, especially by those affecting RF_{CH4} (Etminan et al., 2016). This is illustrated by the earlier RF calculations for KAL (Mathijssen et al., 2017) and LOM (Mathijssen, 2016), which resulted in present-day RF values that were ca. 0.4 nW m^{-2} ha^{-1} lower than in the current study. The remaining difference can be explained by the fact that SII, KAL and LOM had only slowly accumulated C over the Holocene and thus have lower average aCAR of 12.5, 8.9 and 6.3 g C m^{-2} $year^{-1}$, respectively, than the baseline flux densities of ca. 16 g C m^{-2} $year^{-1}$ used by Frolking and Roulet (2007). Additionally, the CH_4 flux densities at our sites were higher than those (ca. 6 g CH_4-C m^{-2} $year^{-1}$) of Frolking and Roulet (2007). Our sites also exhibited low C accumulation rates compared with the mean northern peatland rate of 22.9 ± 2.0 g C m^{-2} $year^{-1}$ (Loisel et al., 2014) and the mean Finnish subarctic fen rate of 16.8 g C m^{-2} $year^{-1}$ (Turunen et al., 2002), and thus may not represent the average northern peatland. However, it should be noted that our RF reconstructions of individual peatlands, with relatively detailed data of C dynamics throughout their development, contain uncertainties of a similar magnitude to those involved in the diverse flux scenarios assumed by Frolking and Roulet (2007). This suggests that the uncertainties in large-scale RF reconstructions derived from peatland data syntheses will be significantly larger than in these simulations.

The persistently positive RF of LOM, resulting from a low C accumulation rate in combination with substantial CH_4 emissions, illustrates that even though a northern peatland has acted as a persistent sink of atmospheric CO_2, it overall may have a climate warming effect. It must be noted that LOM is a fertile valley fen, in which a constant nutrient flow maintains the CH_4 emissions that are relatively high (Zhang et al., 2020) in comparison with net CO_2 uptake (Aurela et al., 2015). In addition, as shown by our results for SII and KAL, there have been extended warming periods during an early phase of peatland development. Even when taking into account the average fluxes of northern peatlands (Loisel et al., 2014), and their negative RF over the Holocene (Frolking & Roulet, 2007), short-term changes in peatland functioning can have large impacts on RF. For example, seen over a time window of 100 year, permafrost thaw in boreal wetlands is estimated to increase RF by 0.02–0.1 nW m^{-2} ha^{-1} (Helbig et al., 2017), and land-use changes may increase RF by as much as 1 nW m^{-2} ha^{-1} (Petrescu et al., 2015). The results of the current study show that such disturbances could potentially counteract the entire negative RF generated by a 10,000 year old peatland.

4.4 | Impact on interpretation of peatland-climate feedback

The present-day RF depends on the present-day fluxes of CH_4 and the cumulative effect of past CO_2 fluxes, but our results show that the method selected to reconstruct CO_2 flux densities (aCAR vs. NCB) has very little effect on the present-day RF, provided we can accurately estimate the present-day total C stock. The different RF trajectories and earlier uptake of CO_2 in the NCB compared with aCAR approach did not lead to diverging present-day RF values. While our present-day RF estimates showed substantial uncertainty also with respect to CH_4 flux estimation, in principle the present-day CH_4 emissions are fairly easy to constrain by flux measurements (Turetsky et al., 2014) and the total C stocks by assessments of peat coverage, depth and C content (Yu, 2012). Hence, estimations of the peatland-scale present-day RF would mainly depend on an accurate reconstruction of lateral expansion. Contrary to the present-day RF, a reconstruction of peatland RF back in time, and the assessment of its function as peatland-climate feedback in the past, depends heavily on the approach adopted to reconstruct C uptake rates, and to a lesser extent on the rate of lateral peatland expansion and the assumptions of CH_4 fluxes in the past (Figures 5 and 6).

It is important to note that the three sites studied here contained 9 to 19 basal dates that were used as a basis for reconstructing their lateral expansion. This many basal dates are typically not available for many peatland sites around the world. In a global reconstruction of peat expansion, Korhola et al. (2010) collected basal dates of over 2200 sites, of which 138 had more than three dates, and only 51 sites contained seven or more basal dates. The number of basal dates necessary to accurately reconstruct peatland expansion increases with peat initiation age, peatland size and complexity. This means that for many peatlands with fewer basal dates than were available for the three sites studied here, the uncertainty of lateral expansion rates would play an even larger role in assessing uncertainties in both the present-day and reconstructed RF. From our results, it seems reasonable to suggest that for sites with few basal dates the uncertainty in RF due to uncertain expansion patterns could be as large as 50%, which has not been taken into consideration in previous estimations of northern peatland Holocene RF (Frolking & Roulet, 2007; Wang et al., 2009).

4.5 | Unaccounted uncertainties

This study does not offer an exhaustive overview of the uncertainties involved in reconstructing the C-balance and related RF of peatlands but adopts the available measurement data from the study sites. If, instead, one would make the decision to return to the site and take more, or other type of, measurements, more sources of uncertainties could be tackled, which now lie outside the scope of this study. Among these would be the number and distribution of basal peat ages used to reconstruct peatland expansion. As the rate of lateral expansion varies within a site, depending on local factors such as topography (Korhola, 1994), the total number and distribution of basal ages necessary to gain an accurate expansion reconstruction would vary among peatland sites. It would be an interesting modelling exercise to test how the uncertainty in expansion pattern depends on the number and distribution of basal ages.

The number and location of the analysed peat cores will also have an effect on the reconstructed C uptake and CH_4 emissions, since C accumulation rates can vary significantly within a site (Korhola et al., 1995; Piilo et al., 2020), and so can water table depth and the associated vegetation and CH_4 emission rates (Turetsky et al., 2014). However, peatland studies containing multiple cores that are analysed in detail are rare, since this is a very time-consuming task. Furthermore, a reconstruction of past CH_4 emissions would ideally also take into account paleotemperatures, given that during warmer temperatures higher CH_4 emissions are expected irrespective of peatland vegetation type (Loisel et al., 2017). Lastly, in all three sites the fate of C which is lost from the peat through lateral flow is not taken into account, assuming that this returns to the atmosphere relatively quickly (Evans et al., 2016). However, if dissolved organic C leached from the peatland would be immobilized subsequently (McKnight et al., 2002), it could be considered to contribute to the long-term C accumulation of the peatland, further decreasing its RF.

The ages of peat layers are commonly analysed using radiocarbon dating and may have uncertainty ranges of up to ±200 year (Nilsson et al., 2001). Additional inaccuracy in peat ages could arise from contamination with 'old' or 'young' C in the analysed material, that is, uptake of CO_2 originating from decomposition of older material or the presence of roots belonging to vegetation growing at the location much later than the deposition of the studied layer, respectively. Varying ^{14}C fractionation among different species and plant tissue types could further decrease the precision of radiocarbon dates (Nilsson et al., 2001; Väliranta et al., 2014). However, these issues can be avoided by dating similar material across the studied samples, preferably *Sphagnum* remains (Nilsson et al., 2001). The remaining chronological uncertainty of a few hundred years should not have a major effect on RF reconstructions spanning multiple thousand years.

5 | CONCLUSION

In this study we set out to investigate the effects on the modelled RF of differing approaches to reconstruct C uptake, methane emissions and lateral peat expansion throughout a peatland's lifetime. The early- to mid-lifetime RF of peatlands was heavily affected by these choices, except that adding the effect of C lost through peat fires did not result in a major effect. For most of the Holocene a peatland's estimated net RF could be either positive or negative, depending on the approach adopted to reconstruct the C fluxes and peat expansion. Using the NCB model instead of the concept of aCAR, or assuming early versus late peat expansion, could change the estimated timing of the switchover from positive to negative RF by several thousand years. Furthermore, an assumption of high past methane emissions can cause the peatland RF to never turn negative despite sustained CO_2 uptake during the Holocene.

Even for estimating the present-day RF, we need data for the whole development history due to sustained sequestration of atmospheric CO_2. In this case, however, the uncertainties are mainly limited to the estimation of lateral expansion patterns. This is because cumulative C uptake and present-day methane emissions can be constrained by the present-day C stock and methane flux measurements at the sites, respectively. Hence, if one's aim is to estimate a peatland's present-day RF status only, it seems sufficient to base calculations on the present-day C stock, methane emission rate and peat initiation age, and obtain enough basal age estimates to accurately reconstruct the development of peatland coverage. However, if one is interested in the development of peatlands' RF over time since peatland initiation, more details are necessary concerning the chronology of peat C accumulation and probable past methane emission, and the inherent uncertainty in these factors should be taken into account in reconstructions of RF.

ACKNOWLEDGEMENTS

This research has been supported by the Academy of Finland (grant numbers 296423; 330840; 337550); University of Helsinki, research funding; Finnish Cultural Foundation; Ministry of Transport and Communication through ICOS-Finland (ICOS-ERIC: 281250; ICOS-Finland: 281255). Open access funding enabled and organized by Projekt DEAL.

CONFLICT OF INTEREST

The authors have no conflict of interest to declare.

DATA AVAILABILITY STATEMENT

The data that support the findings of this study are openly available in Zenodo at https://doi.org/10.5281/zenodo.6241493. The detailed description of the RF model used in this study can be found in Supporting Information.

ORCID

Paul J. H. Mathijssen https://orcid.org/0000-0002-0288-3201
Juha-Pekka Tuovinen https://orcid.org/0000-0001-7857-036X
Annalea Lohila https://orcid.org/0000-0003-3541-672X
Minna Väliranta https://orcid.org/0000-0003-0129-7240
Eeva-Stiina Tuittila https://orcid.org/0000-0001-8861-3167

REFERENCES

Alekseychik, P., Korrensalo, A., Mammarella, I., Launiainen, S., Tuittila, E.-S., Korpela, I., & Vesala, T. (2021). Carbon balance of a Finnish bog: Temporal variability and limiting factors based on 6 years of eddy-covariance data. *Biogeosciences*, *18*(16), 4681–4704. https://doi.org/10.5194/bg-18-4681-2021

Aurela, M. A., Lohila, A., Tuovinen, J.-P., Hatakka, J., Penttilä, T., & Laurila, T. (2015). Carbon dioxide and energy flux measurements in four northern-boreal ecosystems at Pallas. *Boreal Environment Research*, *20*, 455–473. https://pdfs.semanticscholar.org/63e2/c33e0adadb0c8bc18633b9b1d89c9c6ed4bc.pdf

Aurela, M. A., Lohila, A., Tuovinen, J.-P., Hatakka, J., Riutta, T., & Laurila, T. (2009). Carbon dioxide exchange on a northern boreal fen. *Boreal Environment Research*, *14*, 699–710. https://helda.helsinki.fi/bitstream/10138/233552/1/ber14-4-699.pdf

Aurela, M. A., Riutta, T., Laurila, T., Tuovinen, J.-P., Vesala, T., Tuittila, E.-S., Rinne, J., Haapanala, S., & Laine, J. (2007). CO_2 exchange of a sedge fen in southern Finland-the impact of a drought period. *Tellus B: Chemical and Physical Meteorology*, *59*(5), 826–837. https://doi.org/10.1111/j.1600-0889.2007.00309.x

Badorek, T., Tuittila, E.-S., Ojanen, P., & Minkkinen, K. (2011). Forest floor photosynthesis and respiration in a drained peatland forest in southern Finland. *Plant Ecology & Diversity*, *4*(2–3), 227–241. https://doi.org/10.1080/17550874.2011.644344

Beilman, D. W., MacDonald, G. M., Smith, L. C., & Reimer, P. J. (2009). Carbon accumulation in peatlands of West Siberia over the last 2000 years. *Global Biogeochemical Cycles*, *23*(1). https://doi.org/10.1029/2007GB003112

Benscoter, B. W., & Wieder, R. K. (2003). Variability in organic matter lost by combustion in a boreal bog during the 2001 Chisholm fire. *Canadian Journal of Forest Research*, *33*(12), 2509–2513. https://doi.org/10.1139/x03-162

Bubier, J. L., Moore, T. R., & Juggins, S. (1995). Predicting methane emission from bryophyte distribution in northern Canadian Peatlands. *Ecology*, *76*(3), 677–693. https://doi.org/10.2307/1939336

Clymo, R. S., Turunen, J., & Tolonen, K. (1998). Carbon accumulation in Peatland. *Oikos*, *81*(2), 368–388. https://doi.org/10.2307/3547057

Cooper, M. D. A., Estop-Aragonés, C., Fisher, J. P., Thierry, A., Garnett, M. H., Charman, D. J., Murton, J. B., Phoenix, G. K., Treharne, R., Kokelj, S. V., Wolfe, S. A., Lewkowicz, A. G., Williams, M., & Hartley, I. P. (2017). Limited contribution of permafrost carbon to methane release from thawing peatlands. *Nature Climate Change*, *7*(7), 507–511. https://doi.org/10.1038/nclimate3328

Couwenberg, J., Thiele, A., Tanneberger, F., Augustin, J., Bärisch, S., Dubovik, D., Liashchynskaya, N., Michaelis, D., Minke, M., Skuratovich, A., & Joosten, H. (2011). Assessing greenhouse gas emissions from peatlands using vegetation as a proxy. *Hydrobiologia*, *674*(1), 67–89. https://doi.org/10.1007/s10750-011-0729-x

Dommain, R., Frolking, S., Jeltsch-Thömmes, A., Joos, F., Couwenberg, J., & Glaser, P. H. (2018). A radiative forcing analysis of tropical peatlands before and after their conversion to agricultural plantations. *Global Change Biology*, *24*(11), 5518–5533. https://doi.org/10.1111/gcb.14400

Dorrepaal, E., Toet, S., van Logtestijn, R. S. P., Swart, E., van de Weg, M. J., Callaghan, T. V., & Aerts, R. (2009). Carbon respiration from subsurface peat accelerated by climate warming in the subarctic. *Nature*, *460*(7255), 616–619. https://doi.org/10.1038/nature08216

Etminan, M., Myhre, G., Highwood, E. J., & Shine, K. P. (2016). Radiative forcing of carbon dioxide, methane, and nitrous oxide: A significant revision of the methane radiative forcing. *Geophysical Research Letters*, *43*(24), 12614–12623. https://doi.org/10.1002/2016GL071930

Evans, C. D., Renou-Wilson, F., & Strack, M. (2016). The role of waterborne carbon in the greenhouse gas balance of drained and re-wetted peatlands. *Aquatic Sciences*, *78*(3), 573–590. https://doi.org/10.1007/s00027-015-0447-y

Fan, Z., David McGuire, A., Turetsky, M. R., Harden, J. W., Michael Waddington, J., & Kane, E. S. (2013). The response of soil organic carbon of a rich fen peatland in interior Alaska to projected climate change. *Global Change Biology*, *19*(2), 604–620. https://doi.org/10.1111/gcb.12041

Freeman, C., Lock, M. A., & Reynolds, B. (1993). Fluxes of CO_2, CH_4 and N_2O from a Welsh peatland following simulation of water table draw-down: Potential feedback to climatic change. *Biogeochemistry*, *19*(1), https://doi.org/10.1007/BF00000574

Frolking, S., & Roulet, N. T. (2007). Holocene radiative forcing impact of northern peatland carbon accumulation and methane emissions. *Global Change Biology*, *13*(5), 1079–1088. https://doi.org/10.1111/j.1365-2486.2007.01339.x

Frolking, S., Roulet, N., & Fuglestvedt, J. (2006). How northern peatlands influence the Earth's radiative budget: Sustained methane emission versus sustained carbon sequestration. *Journal of Geophysical Research*, *111*(G1), 423. https://doi.org/10.1029/2005JG000091

Frolking, S., Talbot, J., & Subin, Z. M. (2014). Exploring the relationship between peatland net carbon balance and apparent carbon accumulation rate at century to millennial time scales. *The Holocene*, *24*(9), 1167–1173. https://doi.org/10.1177/0959683614538078

Gorham, E. (1991). Northern peatlands: Role in the carbon cycle and probable responses to climatic warming. *Ecological Applications*, *1*(2), 182–195. https://doi.org/10.2307/1941811

Gray, A., Levy, P. E., Cooper, M. D. A., Jones, T., Gaiawyn, J., Leeson, S. R., Ward, S. E., Dinsmore, K. J., Drewer, J., Sheppard, L. J., Ostle, N. J., Evans, C. D., Burden, A., & Zieliński, P. (2013). Methane indicator values for peatlands: A comparison of species and functional groups. *Global Change Biology*, *19*(4), 1141–1150. https://doi.org/10.1111/gcb.12120

Helbig, M., Chasmer, L. E., Kljun, N., Quinton, W. L., Treat, C. C., & Sonnentag, O. (2017). The positive net radiative greenhouse gas forcing of increasing methane emissions from a thawing boreal forest-wetland landscape. *Global Change Biology*, *23*(6), 2413–2427. https://doi.org/10.1111/gcb.13520

Juottonen, H., Kieman, M., Fritze, H., Hamberg, L., Laine, A. M., Merilä, P., Peltoniemi, K., Putkinen, A., & Tuittila, E.-S. (2021). Integrating decomposers, methane-cycling microbes and ecosystem carbon fluxes along a peatland successional gradient in a land uplift region. *Ecosystems*, 1–16. https://doi.org/10.1007/s10021-021-00713-w

Kleinen, T., Brovkin, V., & Schuldt, R. J. (2012). A dynamic model of wetland extent and peat accumulation: Results for the Holocene. *Biogeosciences*, *9*(1), 235–248. https://doi.org/10.5194/bg-9-235-2012

Köhler, P., Nehrbass-Ahles, C., Schmitt, J., Stocker, T. F., & Fischer, H. (2017). A 156 kyr smoothed history of the atmospheric greenhouse gases CO_2, CH_4, and N_2O and their radiative forcing. *Earth System Science Data*, *9*(1), 363–387. https://doi.org/10.5194/essd-9-363-2017

Korhola, A. (1994). Radiocarbon evidence for rates of lateral expansion in raised mires in southern Finland. *Quaternary Research*, *42*(3), 299–307. https://doi.org/10.1006/qres.1994.1080

Korhola, A., Ruppel, M., Seppä, H., Väliranta, M., Virtanen, T., & Weckström, J. (2010). The importance of northern peatland expansion to the late-Holocene rise of atmospheric methane. *Quaternary Science Reviews*, *29*(5–6), 611–617. https://doi.org/10.1016/j.quascirev.2009.12.010

Korhola, A., Tolonen, K., Turunen, J., & Jungner, H. (1995). Estimating long-term carbon accumulation rates in boreal peatlands by radiocarbon dating. *Radiocarbon*, *37*(2), 575–584. https://doi.org/10.1017/S0033822200031064

Korrensalo, A., Männistö, E., Alekseychik, P., Mammarella, I., Rinne, J., Vesala, T., & Tuittila, E.-S. (2018). Small spatial variability in methane emission measured from a wet patterned boreal bog. *Biogeosciences*, *15*(6), 1749–1761. https://doi.org/10.5194/bg-15-1749-2018

Koskinen, M., Minkkinen, K., Ojanen, P., Kämäräinen, M., Laurila, T., & Lohila, A. (2014). Measurements of CO_2 exchange with an automated chamber system throughout the year: Challenges in measuring night-time respiration on porous peat soil. *Biogeosciences*, *11*(2), 347–363. https://doi.org/10.5194/bg-11-347-2014

Laine, A. M., Bubier, J. L., Riutta, T., Nilsson, M. B., Moore, T. R., Vasander, H., & Tuittila, E.-S. (2012). Abundance and composition of plant biomass as potential controls for mire net ecosytem CO_2 exchange. *Botany-Botanique*, *90*(1), 63–74. https://doi.org/10.1139/b11-068

Langeveld, C. A., Segers, R., Dirks, B. O. M., van den Dasselaar, A. P., Velthof, G. L., & Hensen, A. (1997). Emissions of CO_2, CH_4 and N_2O from pasture on drained peat soils in the Netherlands. *European Journal of Agronomy*, *7*(1), 35–42. https://doi.org/10.1016/S1161-0301(97)00036-1

Leppälä, M., Laine, A. M., Seväkivi, M.-L., & Tuittila, E.-S. (2011). Differences in CO_2 dynamics between successional mire plant communities during wet and dry summers. *Journal of Vegetation Science*, *22*(2), 357–366. https://doi.org/10.1111/j.1654-1103.2011.01259.x

Leppälä, M., Oksanen, J., & Tuittila, E.-S. (2011). Methane flux dynamics during mire succession. *Oecologia*, *165*(2), 489–499. https://doi.org/10.1007/s00442-010-1754-6

Limpens, J., Berendse, F., Blodau, C., Canadell, J. G., Freeman, C., Holden, J., Roulet, N., Rydin, H., & Schaepman-Strub, G. (2008). Peatlands and the carbon cycle: from local processes to global implications—A synthesis. *Biogeosciences*, *5*(5), 1475–1491. https://doi.org/10.5194/bg-5-1475-2008

Lohila, A., Minkkinen, K., Aurela, M. A., Tuovinen, J.-P., Penttilä, T., Ojanen, P., & Laurila, T. (2011). Greenhouse gas flux measurements in a forestry-drained peatland indicate a large carbon sink. *Biogeosciences*, *8*(11), 3203–3218. https://doi.org/10.5194/bg-8-3203-2011

Lohila, A., Minkkinen, K., Laine, J., Savolainen, I., Tuovinen, J.-P., Korhonen, L., Laurila, T., Tietäväinen, H., & Laaksonen, A. (2010). Forestation of boreal peatlands: Impacts of changing albedo and greenhouse gas fluxes on radiative forcing. *Journal of Geophysical Research*, *115*(G4), 311. https://doi.org/10.1029/2010JG001327

Loisel, J., van Bellen, S., Pelletier, L., Talbot, J., Hugelius, G., Karran, D., Yu, Z., Nichols, J. E., & Holmquist, J. (2017). Insights and issues with estimating northern peatland carbon stocks and fluxes since the Last Glacial Maximum. *Earth-Science Reviews*, *165*, 59–80. https://doi.org/10.1016/j.earscirev.2016.12.001

Loisel, J., & Yu, Z. (2013). Recent acceleration of carbon accumulation in a boreal peatland, south central Alaska. *Journal of Geophysical Research: Biogeosciences*, *118*(1), 41–53. https://doi.org/10.1029/2012JG001978

Loisel, J., Yu, Z., Beilman, D. W., Camill, P., Alm, J., Amesbury, M. J., Anderson, D., Andersson, S., Bochicchio, C., Barber, K., Belyea, L. R., Bunbury, J., Chambers, F. M., Charman, D. J., De Vleeschouwer, F., Fiałkiewicz-Kozieł, B., Finkelstein, S. A., Gałka, M., Garneau, M., … Zhou, W. (2014). A database and synthesis of northern peatland soil properties and Holocene carbon and nitrogen accumulation. *The Holocene*, *24*(9), 1028–1042. https://doi.org/10.1177/0959683614538073

Mäkilä, M. (1997). Holocene lateral expansion, peat growth and carbon accumulation on Haukkasuo, a raised bog in southeastern Finland. *Boreas*, *26*(1), 1–14. https://doi.org/10.1111/j.1502-3885.1997.tb00647.x

Mäkilä, M., & Moisanen, M. (2007). Holocene lateral expansion and carbon accumulation of Luovuoma, a northern fen in Finnish Lapland. *Boreas*, *36*(2), 198–210. https://doi.org/10.1111/j.1502-3885.2007.tb01192.x

Männistö, E., Korrensalo, A., Alekseychik, P., Mammarella, I., Peltola, O., Vesala, T., & Tuittila, E.-S. (2019). Multi-year methane ebullition measurements from water and bare peat surfaces of a patterned boreal bog. *Biogeosciences*, *16*(11), 2409–2421. https://doi.org/10.5194/bg-16-2409-2019

Martikainen, P. J., Nykänen, H., Crill, P., & Silvola, J. (1993). Effect of a lowered water table on nitrous oxide fluxes from northern peatlands. *Nature*, *366*(6450), 51–53. https://doi.org/10.1038/366051a0

Mathijssen, P. J. H. (2016). *Holocene carbon dynamics and atmospheric radiative forcing of different types of peatlands in Finland* [Doctoral dissertation, University of Helsinki]. helda.helsinki.fi. https://helda.helsinki.fi/bitstream/10138/161250/1/HOLOCENE.pdf

Mathijssen, P., Tuovinen, J.-P., Lohila, A., Tuittila, E.-S., & Väliranta, M. (2022). Data used to reconstruct carbon dynamics of Siikaneva, Kalevansuo and Lompolojänkkä. [Data set]. *Zenodo*. https://doi.org/10.5281/zenodo.6241493

Mathijssen, P. J. H., Kähkölä, N., Tuovinen, J.-P., Lohila, A., Minkkinen, K., Laurila, T., & Väliranta, M. (2017). Lateral expansion and carbon exchange of a boreal peatland in Finland resulting in 7000 years of positive radiative forcing. *Journal of Geophysical Research: Biogeosciences*, *122*(3), 562–577. https://doi.org/10.1002/2016JG003749

Mathijssen, P. J. H., Tuovinen, J.-P., Lohila, A., Aurela, M. A., Juutinen, S., Laurila, T., Niemelä, E., Tuittila, E.-S., & Väliranta, M. (2014). Development, carbon accumulation, and radiative forcing of a subarctic fen over the Holocene. *The Holocene*, *24*(9), 1156–1166. https://doi.org/10.1177/0959683614538072

Mathijssen, P. J. H., Väliranta, M., Korrensalo, A., Alekseychik, P., Vesala, T., Rinne, J., & Tuittila, E.-S. (2016). Reconstruction of Holocene carbon dynamics in a large boreal peatland complex, southern Finland. *Quaternary Science Reviews*, *142*, 1–15. https://doi.org/10.1016/j.quascirev.2016.04.013

McKnight, D. M., Hornberger, G. M., Bencala, K. E., & Boyer, E. W. (2002). In-stream sorption of fulvic acid in an acidic stream: A stream-scale transport experiment. *Water Resources Research*, *38*(1), 6-1–6-12. https://doi.org/10.1029/2001WR000269

Mikaloff-Fletcher, S. E., Tans, P. P., Bruhwiler, L. M., Miller, J. B., & Heimann, M. (2004). CH_4 sources estimated from atmospheric observations of CH_4 and its $^{13}C/^{12}C$ isotopic ratios: 1. Inverse modeling of source processes. *Global Biogeochemical Cycles*, *18*(4). https://doi.org/10.1029/2004GB002223

Minkkinen, K., & Ojanen, P. (2013). *Pohjois-Pohjanmaan turvemaiden kasvihuonekaasutaseet* (Metlan työraportteja No. 258).

Minkkinen, K., Ojanen, P., Penttilä, T., Aurela, M. A., Laurila, T., Tuovinen, J.-P., & Lohila, A. (2018). Persistent carbon sink at a boreal drained bog forest. *Biogeosciences*, *15*(11), 3603–3624. https://doi.org/10.5194/bg-15-3603-2018

Myhre, G., Shindell, D., Bréon, F.-M., Collins, W., Fuglestvedt, J., Huang, J., Koch, D., Lamarque, J.-F., Lee, D., & Mendoza, B. (2013). Anthropogenic and Natural Radiative Forcing. In T. F. Stocker, D. Qin, G.-K. Plattner, M. Tignor, S. K. Allen, J. Boschung, A. Nauels, Y. Xia, V. Bex, & P. M. Midgley (Eds.), *Climate change 2013: The physical science basis. Contribution of working group I to the fifth assessment report of the intergovernmental panel on climate change* (pp. 659–740). Cambridge University Press. https://doi.org/10.1017/CBO9781107415324.018

Nilsson, M. B., Klarqvist, M., Bohlin, E., & Possnert, G. (2001). Variation in ^{14}C age of macrofossils and different fractions of minute peat samples dated by AMS. *The Holocene*, *11*(5), 579–586. https://doi.org/10.1191/095968301680223521

Ojanen, P., Minkkinen, K., Lohila, A., Badorek, T., & Penttilä, T. (2012). Chamber measured soil respiration: A useful tool for estimating the carbon balance of peatland forest soils? *Forest Ecology and Management*, *277*, 132–140. https://doi.org/10.1016/j.foreco.2012.04.027

Petrescu, A. M. R., Lohila, A., Tuovinen, J.-P., Baldocchi, D. D., Desai, A. R., Roulet, N. T., Vesala, T., Dolman, A. J., Oechel, W. C., Marcolla, B., Friborg, T., Rinne, J., Matthes, J. H., Merbold, L., Meijide, A., Kiely, G., Sottocornola, M., Sachs, T., Zona, D., … Cescatti, A. (2015). The uncertain climate footprint of wetlands under human pressure. *Proceedings of the National Academy of Sciences of the United States of America*, *112*(15), 4594–4599. https://doi.org/10.1073/pnas.1416267112

Pihlatie, M., Kiese, R., Brüggemann, N., Butterbach-Bahl, K., Kieloaho, A.-J., Laurila, T., Lohila, A., Mammarella, I., Minkkinen, K., Penttilä, T., Schönborn, J., & Vesala, T. (2010). Greenhouse gas fluxes in a drained peatland forest during spring frost-thaw event. *Biogeosciences*, *7*(5), 1715–1727. https://doi.org/10.5194/bg-7-1715-2010

Piilo, S. R., Korhola, A., Heiskanen, L., Tuovinen, J.-P., Aurela, M., Juutinen, S., Marttila, H., Saari, M., Tuittila, E.-S., Turunen, J., & Väliranta, M. (2020). Spatially varying peatland initiation, Holocene development, carbon accumulation patterns and radiative forcing within a subarctic fen. *Quaternary Science Reviews*, *248*, 106596. https://doi.org/10.1016/j.quascirev.2020.106596

Repo, M. E., Susiluoto, S., Lind, S. E., Jokinen, S., Elsakov, V., Biasi, C., Virtanen, T., & Martikainen, P. J. (2009). Large N_2O emissions from cryoturbated peat soil in tundra. *Nature Geoscience*, *2*(3), 189–192. https://doi.org/10.1038/ngeo434

Rinne, J., Riutta, T., Pihlatie, M., Aurela, M. A., Haapanala, S., Tuovinen, J.-P., Tuittila, E.-S., & Vesala, T. (2007). Annual cycle of methane emission from a boreal fen measured by the eddy covariance technique. *Tellus B: Chemical and Physical Meteorology*, *59*(3), 449–457. https://doi.org/10.1111/j.1600-0889.2007.00261.x

Riutta, T., Laine, J., Aurela, M. A., Rinne, J., Vesala, T., Laurila, T., Haapanala, S., Pihlatie, M., & Tuittila, E.-S. (2007). Spatial variation in plant community functions regulates carbon gas dynamics in a boreal fen ecosystem. *Tellus B: Chemical and Physical Meteorology*, *59*(5), 838–852. https://doi.org/10.1111/j.1600-0889.2007.00302.x

Rydin, H., & Jeglum, J. K. (2013). *The biology of peatlands. The biology of habitats series* (2nd ed.). Oxford University Press.

Turetsky, M. R., Kotowska, A., Bubier, J. L., Dise, N. B., Crill, P., Hornibrook, E. R. C., Minkkinen, K., Moore, T. R., Myers-Smith, I. H., Nykänen, H., Olefeldt, D., Rinne, J., Saarnio, S., Shurpali, N. J., Tuittila, E.-S., Waddington, J. M., White, J. R., Wickland, K. P., & Wilmking, M. (2014). A synthesis of methane emissions from 71 northern, temperate, and subtropical wetlands. *Global Change Biology*, *20*(7), 2183–2197. https://doi.org/10.1111/gcb.12580

Turetsky, M. R., & Wieder, R. K. (2001). A direct approach to quantifying organic matter lost as a result of peatland wildfire. *Canadian Journal of Forest Research*, *31*(2), 363–366. https://doi.org/10.1139/x00-170

Turunen, J., Tomppo, E., Tolonen, K., & Reinikainen, A. (2002). Estimating carbon accumulation rates of undrained mires in Finland–application to boreal and subarctic regions. *The Holocene*, *12*(1), 69–80. https://doi.org/10.1191/0959683602hl522rp

Väliranta, M., Oinonen, M., Seppä, H., Korkonen, S., Juutinen, S., & Tuittila, E.-S. (2014). Unexpected problems in AMS ^{14}C dating of fen peat. *Radiocarbon*, *56*(1), 95–108. https://doi.org/10.2458/56.16917

Wang, Y., Roulet, N. T., Frolking, S., & Mysak, L. A. (2009). The importance of Northern Peatlands in global carbon systems during the Holocene. *Climate of the Past*, *5*(4), 683–693. https://doi.org/10.5194/cp-5-683-2009

Young, D. M., Baird, A. J., Charman, D. J., Evans, C. D., Gallego-Sala, A. V., Gill, P. J., Hughes, P. D. M., Morris, P. J., & Swindles, G. T. (2019). Misinterpreting carbon accumulation rates in records from near-surface peat. *Scientific Reports*, *9*(1), 17939. https://doi.org/10.1038/s41598-019-53879-8

Yu, Z. (2011). Holocene carbon flux histories of the world's peatlands: Global carbon-cycle implications. *The Holocene*, *21*(5), 761–774. https://doi.org/10.1177/0959683610386982

Yu, Z. (2012). Northern peatland carbon stocks and dynamics: A review. *Biogeosciences*, *9*(10), 4071–4085. https://doi.org/10.5194/bg-9-4071-2012

Yu, Z., Loisel, J., Brosseau, D. P., Beilman, D. W., & Hunt, S. J. (2010). Global peatland dynamics since the last glacial maximum. *Geophysical Research Letters*, *37*(13). https://doi.org/10.1029/2010GL043584

Zhang, H., Tuittila, E.-S., Korrensalo, A., Räsänen, A., Virtanen, T., Aurela, M. A., Penttilä, T., Laurila, T., Gerin, S., Lindholm, V., & Lohila, A. (2020). Water flow controls the spatial variability of methane emissions in a northern valley fen ecosystem. *Biogeosciences*, *17*(23), 6247–6270. https://doi.org/10.5194/bg-17-6247-2020

SUPPORTING INFORMATION

Additional supporting information may be found in the online version of the article at the publisher's website.

How to cite this article: Mathijssen, P. J. H., Tuovinen, J.-P., Lohila, A., Väliranta, M., & Tuittila, E.-S. (2022). Identifying main uncertainties in estimating past and present radiative forcing of peatlands. *Global Change Biology*, *28*, 4069–4084. https://doi.org/10.1111/gcb.16189